Article

Not peer-reviewed version

Tq-Diagram Computing Algorithm for the Multi-Flow Heat Exchanger

Andrii Rozhentsev *

Posted Date: 14 November 2025

doi: 10.20944/preprints202511.1092.v1

Keywords: multi-flow heat exchanger; T-Q diagram; thermodynamic modeling; pinch analysis; algorithm; process simulation; cryogenic processes; second law of thermodynamics; entropy generation minimization; heat exchanger network

Preprints.org (www.preprints.org) | NOT PEER-REVIEWED | Posted: 14 November 2025 doi:10.20944/preprints202511.1092.v1

Article

Tq-Diagram Computing Algorithm for the Multi-Flow Heat Exchanger

Andrey Rozhentsev

Nuclear Department, National R&D Institute for Cryogenic and Isotopic Technologies, Rm. Valcea, str. Uzinei nr. 4, Romania; andrii.rozhentsev@icsi.ro or rozhentsev.av@gmail.com

Abstract

The study given considers a technique for computing the qT-diagram of a multi-flow heat exchanger with an arbitrary number of flows. The specified parameters of the computation are the temperature, pressure, mass rate of all hot and cold flows at the heat exchanger inlet port, and the value of the lowest allowed temperature difference between the flows. The last parameter establishes the heat exchanger's overall thermodynamic efficiency. The algorithm for calculating the qT-diagram includes the calculation of the maximum heat content of the flows, the maximum amount of heat that can be transferred in the heat exchanger, and all possible distributions of this heat between the flows. The outlet temperatures of the flows are computed for each heat distribution, and the results are sorted and ranked according to the chosen objective function. The sorted operating modes of the heat exchanger are checked from the point of view of the qT-diagram's operability in accordance with a given criterion. Comparisons with the results of calculations of similar heat exchangers in the HYSYS AspenONE verified the algorithm's accuracy and physical consistency.

Keywords: multi-flow heat exchanger; T-Q diagram; thermodynamic modeling; pinch analysis; algorithm; process simulation; cryogenic processes; second law of thermodynamics; entropy generation minimization; heat exchanger network

---

1. Introduction

Thermal analysis and design of heat exchangers remain among the key problems of engineering thermophysics, particularly in cryogenic and energy systems. The most common engineering tools for such analysis are based on T–Q or T–H diagrams, which relate the temperature of the interacting flows to the amount of transferred heat. These diagrams form the basis of both the classical heat exchanger network (HEN) synthesis methods and modern software packages such as Aspen HYSYS, Aspen Exchanger Design & Rating, HTRI Xchanger Suite, or ANSYS Fluent.

The first formalized methods for analyzing heat exchanger networks trace back to the pioneering work of Hohmann (1971) [1], which laid the groundwork for the seminal works of Linnhoff and Flower (1978) [2]. The latter introduced the pinch analysis technique and the concept of composite curves for two-flow systems, providing an intuitive visualization of thermal interactions and became the foundation for energy-optimal design of exchanger networks. However, the classical pinch methodology is fundamentally limited to two-flow exchangers or equivalent pairwise interactions, where the heat balance can be expressed unambiguously.

In multi-flow heat exchangers (MFHEXs), which are common in cryogenic separation systems, regenerative exchangers, and recuperators with phase transitions, these assumptions fail. Commercial simulation packages such as Aspen HYSYS or HTRI typically treat the problem empirically: users specify temperature differences between the inlet and outlet of each stream, and the program verifies whether the resulting configuration is "operable." In this process, however, no explicit verification of the second law of thermodynamics is performed at every internal section of the exchanger. As a result, the generated T–Q diagrams may formally appear feasible while actually allowing intersections of the flow temperature curves - a physically impossible scenario.

Other approaches, often found in the literature, are based on local heat transfer equations and the numerical integration of differential equations along the exchanger length (e.g., Ghannadzadeh et al., 2020 [3]; Wang & Xu, 2019 [4]). Although these methods can reproduce detailed profiles of temperature and enthalpy, they require prior knowledge of the exchanger geometry, wall properties, and heat transfer coefficients - parameters that are often unknown in the early thermodynamic analysis stage. Consequently, such approaches are not universal and cannot directly determine whether a feasible heat exchange process exists for a given set of inlet flow conditions.

Entropy-based and exergy-based optimization methods (e.g., Bejan, 1997 [5]) address thermodynamic irreversibility explicitly, yet they are also primarily formulated for two-flow systems or rely on approximating multi-stream exchange as a sequence of binary interactions. This again limits their generality and applicability to real MFHEX configurations.

These limitations motivate the development of a universal thermodynamic algorithm capable of constructing T–Q diagrams for arbitrary multi-flow exchangers without invoking heat transfer equations. The algorithm should:

rely solely on the inlet parameters of all flows (temperature, pressure, mass rate, and composition);

include the minimum allowable temperature difference between any flows as a thermodynamic constraint;

avoid using any geometrical or construction data of the exchanger;

ensure strict compliance with the second law of thermodynamics under all flow combinations.

This method offers a powerful tool for process engineers, enabling them to rapidly screen feasible operating modes and identify thermodynamically optimal configurations for MFHEXs during the conceptual design phase. This can lead to significant reductions in both capital and operational costs by ensuring energy-efficient and physically realizable heat exchanger designs from the outset.

The present study introduces such a method. It is based on the direct thermodynamic analysis of the overall energy balance of a multi-flow heat exchanger, introducing the concepts of active and passive flow bundles. The method involves enumerating all admissible distributions of heat contents between flows, followed by ranking and selection according to thermodynamic objective functions - either entropy-based or temperature-based. The obtained T–Q diagrams, when compared with calculations performed in Aspen HYSYS 12.1, show that the proposed algorithm provides high consistency and physical adequacy without requiring any prior assumptions about heat transfer mechanisms or exchanger geometry.

2. Well Defined Case of a Double-Flow Heat Exchanger

The *thermodynamic* computation of flow temperatures at the outlets of a 2-flow counterflow heat exchanger (HEX) is a routine procedure for designing different types of refrigeration and thermal engineering equipment. The reasonable accuracy and simplicity of that approach challenge more precise but far more complicated computations based on a set of differential equations relating to hydraulics and heat transfer.

The calculation's "Thermodynamism" lies in the fact that, for given input flow temperatures T_{in}^h, T_{in}^c, the outlet temperatures T_{out}^h, T_{out}^c are entirely determined by the actual amount of heat Q_{act} transferred in the heat exchanger. This can be thought of as a general application of the first law of thermodynamics to the HEX as a whole, without accounting for the specifics of the heat transfer process and the associated design parameters of the HEX.

In the case of ideal heat exchange without losses, the limit amount of heat Q_{LIM} transferred from hot to cold flow corresponds to the lower of the limit heat content of flows Q_{LIM}^h and Q_{LIM}^c. The term "heat content" refers to the difference in the total enthalpies of the flow at a HEX's inlet and outlet ports. The flows limit heat contents Q_{LIM}^h and Q_{LIM}^c are calculated on the assumption of the equality of the corresponding inlet and outlet temperatures:

$$Q_{LIM} = \min(Q^h_{LIM}(T^h_{in}, T^h_{out\_min} = T^c_{in}),\ Q^c_{LIM}(T^c_{in}, T^c_{out\_max} = T^h_{in}),$$

$$Q^h_{LIM} = \left(h^h(T^h_{in},\ P^h) - h^h(T^h_{out\_min} = T^c_{in},\ P^h)\right)\dot{m}^h, \tag{1}$$

$$Q^c_{LIM} = \left(h^c(T^c_{out\_max} = T^h_{in},\ P^c) - \ h^c(T^c_{in},\ P^c)\right)\dot{m}^c,$$

here and hereafter, mathematical notations like $h(T,P)$ or $T(h,P)$ imply the use of the corresponding equation of state[1].

In the actual real-world scenario case, when irreversible heat exchange losses are to be taken into account, the quantity of heat Q_{act} actually transferred between the TH flows can be defined as a certain fraction of Q_{LIM}:

$$Q_{act} = \varepsilon \cdot Q_{LIM}, \tag{2}$$

where $\varepsilon \in]0..1]$ is the coefficient of heat transfer efficiency and its value is set subjectively ($\varepsilon = 1$ – ideal heat transfer).

It is clear how to calculate the enthalpies and temperatures of the flows at the outlet cross-sections given a known value for Q_{act}:

$$h^h_{out} = h^h(T^h_{in},\ P^h) - \frac{Q_{act}}{\dot{m}^h} \rightarrow T^h_{out} = T^h(h^h_{out},\ P^h)$$
$$h^c_{out} = h^c(T^c_{in},\ P^c) + \frac{Q_{act}}{\dot{m}^c} \rightarrow T^c_{out} = T^c(h^c_{out},\ P^c) \tag{3}$$

The heat exchange efficiency coefficient ε, which was previously provided, is often not employed in engineering calculations to account for losses in the heat exchange process between flows. Instead, the value of the minimum allowable temperature difference at the end of the heat exchanger, ΔT_{end_min}, is used. This indicates that the flow's temperature difference at the heat exchanger's ends can only be more than or equal to ΔT_{end_min}. Using this method, the value of the outlet temperature of ***one*** of the streams may be clearly determined based on the ratio of its limit heat contents:

$$Q^h_{LIM} \geq Q^c_{LIM}: \quad T^c_{out} = T^h_{in} - \Delta T_{end\_min};$$
$$Q^h_{LIM} \leq Q^c_{LIM}: \quad T^h_{out} = T^c_{in} + \Delta T_{end\_min}. \tag{4}$$

Determine Q_{act} and the temperature of the second flow at the heat exchanger's outlet using the outlet temperature of one of the flows (T^h_{out} or T^c_{out}) (see eq. (3)).

Both strategies are equally effective and depend only on the individual. Similar to ε, the particular value of ΔT_{end_min} is selected based on personal preference. The maximum value is constrained by the values of the inlet flow temperatures, while its lowest value is set within (3 .. 6), K. However, when doing numerical computations of the flow temperatures along a HX's length, it may be beneficial to set strict, clear limits on the range of values $\varepsilon \in]0..1]$.

The thermal load Q_{act} (see eq. (3)) uniquely determines the valuesT^h_{out}, T^c_{out} in any of these calculation alternatives, and it is *a priori assumed* (without verification) that the condition:

[1] The NIST REFPROP 10.0 precompiled dynamically linked library is used to calculate the thermodynamic and transport properties of fluids and their mixtures (NIST License for Order # O-0000049481; National Research and Development Institute for Cryogenic and Isotopic Technologies – ICSI, Rm. Valcea, Romania)

 doi:10.20944/preprints202511.1092.v1

$$T_i^h > T_i^c, \ \ \mathrm{i} \in [0, n] \tag{5}$$

holds for each i^{th} cross section of the HEX.

The last assumption is valid for ***a limited number of cases*** when the dependences $T^h(h^h, P^h = const)$ and $T^c(h^c, P^c = const)$ for working substance flows remain close to linear in the corresponding temperature ranges: $[T_{in}^h, T_{out}^h = T_{in}^c]$, $[T_{in}^c, T_{out}^c = T_{in}^h]$. This means that the above-mentioned approach should only be used in situations where there are no phase transitions occurring during the heat exchange process and flow temperature variations of no more than a few tens of degrees.

If the dependences $T^h(h^h, P^h = const)$ or $T^c(h^c, P^c = const)$ are nonlinear in the temperature ranges that are being studied, then computations should be done not only for the flow temperatures T_{out}^h, T_{out}^c at the heat exchanger's outlet but also along the entire length of the heat exchanger, based on the quantity of heat transferred:

$$T_i^h = f(Q_i), \quad T_i^c = f(Q_i), \text{где } \ Q_i \in [0..Q_{act}]. \tag{6}$$

then determining if the requirement $T_i^h - T_i^c > \Delta T_{min}$ has been met.

The *Tq*-diagram of HEX (see *Figure 1*) is the graphical depiction of dependencies (6).

Algorithm to Compute the 2-Flow Heat Exchanger's Tq-Diagram

The *Tq*-diagram of the two-flow HEX must be calculated after figuring out Q_{max} and Q_{act} (eq. (1), (2)) and their corresponding flow temperatures at the HEX's outlets T_{out}^h and T_{out}^c (eq. (3)).

Then the entire HEX is divided along the length into n sections. To ensure that the thermodynamic properties of the flows $T^h(h^h, P^h = const)$ and $T^c(h^c, P^c = const)$ evolve in a nearly linear fashion over each segment, a particular value of n is to be selected.

Usually, n is chosen such that the temperature changes by 5 to 10 degrees *along* a section $\Delta T = T_{i+1} - T_i$, and then the total number of sections n: $n = int(T_{in}^h - T_{in}^c/\Delta T)$. The sections are numbered starting from the inlet port of the cold flow: $h_{i=0}^c = h_{in}^c, h_{i=n}^c = h_{out}^c$; $h_{i=0}^h = h_{out}^h, h_{i=n}^h = h_{in}^h$. The flows' temperatures and enthalpies are then computed for all HEX's sections.

$$h_i^h = h_{in}^h - \frac{Q_{act}}{n \cdot \dot{m}^h} \cdot (n - i), \quad i \in [0..n] \ \ \rightarrow \ T_i^h = T^h(h_i^h, P^h) \tag{7}$$

$$h_i^c = h_{in}^c + \frac{Q_{act}}{n \cdot \dot{m}^c} \cdot i, \qquad i \in [0..n] \ \ \rightarrow \ T_i^c = T^c(h_i^c, P^c) \tag{8}$$

If the temperature difference between the hot and cold flows in each *internal* cross-section of the HEX is greater than a predetermined value ΔT_{min}, then the *Tq*-diagram is deemed to be ***operational*** (the appropriate values of the HEX's ends temperature differences are established earlier; see eq. (3), (4)):

$$T_i^h - T_i^c > \Delta T_{min}, \ \ \mathrm{i} \in]0..n[\tag{9}$$

Figure 1 presents three alternatives for the *Tq*-diagram of two-flow HEX calculated with input data from *Table 1*. Based on the HEX's heat balance (eq. (1)) and idealized conditions of transferring the maximum possible amount of heat in the HEX $Q_{act} = Q_{LIM} =$ 73.2, kW; (eq. (2)) the diagram in Figure 1A was created. In this instance, the condition of a zero-temperature difference between the flows at one of the HEX's ends—here, the cold end—is automatically met. It is believed that the observed intersection of the temperature curves in *Figure 1A* violates the second rule of thermodynamics, indicating that such a process is physically impossible to carry out under any heat transfer scenario. In actuality, it means that under the set initial data, it is impossible to transfer a given quantity of heat Q_{act} from a hot to a cold flow. In this scenario, either the lowest allowable

HEX's end temperature difference ΔT_{end_min} or the coefficient of heat transfer efficiency ε should be decreased in order to lower Q_{act} (see eq. (2), (4)).

Table 1. Initial data for calculating the Tq-diagram of the counterflow HEX.

Flow		Working fluid		Flow parameters at the HEX's inlet ports		
type	index	component	composition mol/mol	Temperature K	Pressure bar	Mass rate kg/h
Hot	1	CH_4	99.973178	225.5	28.11	408.8680
		N_2	0.024569			
		O_2	0.002257			
Cold	1	CH_4	99.969465	127.6473	2.0	1677.9048
		N_2	0.028048			
		O_2	0.002490			

In *Figure 1B*, the Tq-diagram is likewise computed for the idealized heat transfer process in the HEX, but under the condition that $\Delta T_{min} = 0$ (see eq. (9)), which is the minimal allowable value of the temperature difference between the flows in any internal cross-sections. In this instance, $Q_{act} =$ 66.9 kW of heat is transferred in the HEX. This is the maximum quantity of heat Q_{MAX} that can be transferred in the HEX under these initial data without going against the second law of thermodynamics. The operational diagram of the HEX, computed for the constraint ΔT_{min} = 5 K, is shown in *Figure 1C*. The amount of heat transferred in the HEX is Q_{act} = 62.8 kW, or 93% of its maximum value of $Q_{MAX} =$ 66.9 kW.

It is evident that the value of Q_{MAX} but not Q_{LIM} should be the basis for the iterative calculation of both the Tq-diagram and the HEX's efficiency. However, given the constraint $\Delta T_{min} = 0$, the computation of the Q_{MAX} value requires an extensive iterative computation of the Tq-diagram in itself (see (9)). Consequently, the value Q_{LIM} is used as the maximum heat load for calculation of Tq-diagrams employing the concept of the HEX's thermal efficiency ε. This very slightly increases the number of iterations; otherwise, it has no effect on the final computation results. Wherein, the value Q_{MAX} should clearly be used to evaluate the effectiveness of a HEX: $\varepsilon = Q_{act}/Q_{MAX}$.

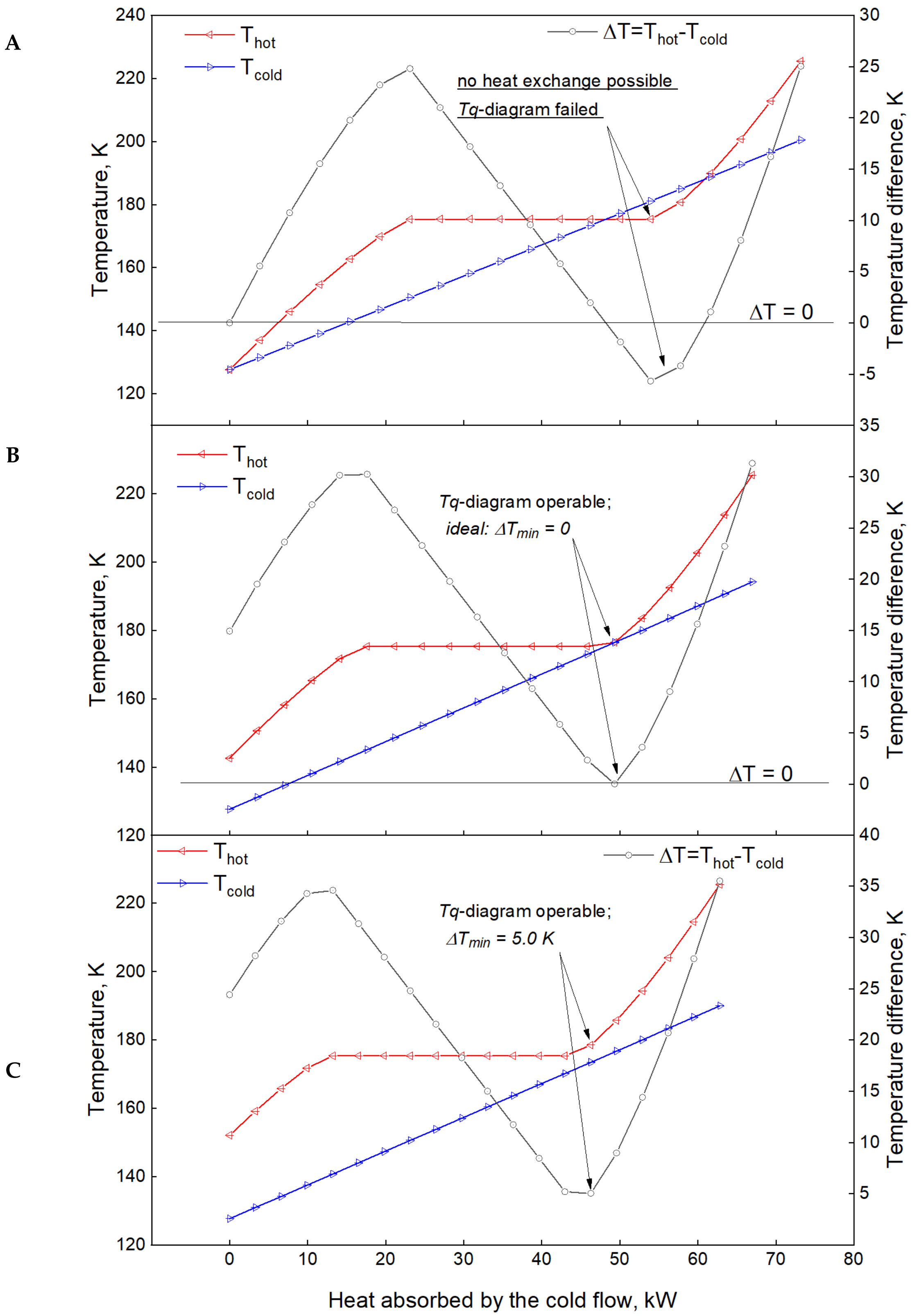

Figure 1. Tq-diagram of the 2-flow counterflow HEX (initial data see Table 1): **A** – given $\Delta T_{end\_min} = 0$ ($\varepsilon = 1.0$); **B** – given $\Delta T_{min} = 0$; **C** – given $\Delta T_{min} = 5.0$ K.

3. A multi-Flow Heat Exchanger Case Study

The above-discussed two-flow heat exchanger is a special case of a multi-flow heat exchanger (MFHEX), where several hot $N^h \geq 1$ and cold $N^c \geq 1$ flows undergo simultaneous heat exchange. The set of all hot flows of a MFHEX will be referred to as a ***hot bundle*** for brevity, and the set of all

Preprints.org (www.preprints.org) | NOT PEER-REVIEWED | Posted: 14 November 2025 doi:10.20944/preprints202511.1092.v1

cold flows as a ***cold bundle***. Calculating the Tq-diagram of a two-flow HEX does not contain any particular difficulties since the amount of heat given off by the hot flow at each heat exchange section is equal to the amount of heat absorbed by the cold flow, either taking into account possible losses or without them in the case of ideal heat exchange. In the thermodynamic calculation of a MFHEX, there is no such unambiguous relationship between the amount of heat transferred between flows, since thermodynamics does not operate with such concepts as heat transfer coefficients and heat transfer surface area. The latter significantly complicates the procedure for calculating the Tq-diagram of MFHEXs.

As in the case of a two-flow HEX, the first step is to determine the amount of heat transferred in the MFHEX ***from all*** hot flows ***to all*** cold flows.

We will assume that each of the N^h hot flows is in the process of heat exchange with each of the N^c cold flows and can only emit heat. To avoid a situation where any of the hot flows may turn out to be colder than any of the cold flows, we accept the assumption that there is a limiting temperature $T^h_{out\_lim}$ for hot flows at the MFHEX's outlet ports. None of the hot flows can have a temperature lower than $T^h_{out\_lim}$, and this temperature will correspond to the temperature of the "hottest" of the cold flows at the MFHEX's inlet ports:

$$T^h_{out\_lim} = max\left(T^c_{i\_in}\right), \;\; i \in [1..\, N^c] \tag{10}$$

Following the same logic, the limiting temperature $T^c_{out\_lim}$ for cold flows at the outlet of the MFHEX will correspond to the temperature of the "coldest" of the hot flows at the inlet to the heat exchanger:

$$T^c_{out\_lim} = min\left(T^h_{j\_in}\right), \;\; j \in [1..\, N^h] \tag{11}$$

The assumption of limiting temperatures $T^h_{out\_lim}$, $T^c_{out\_lim}$ implies the presence of limiting heat contents in flows $Q^h_{i\_lim}$, $Q^c_{j\_lim}$. The values of $Q^h_{i\_lim}$, and $Q^c_{j\_lim}$ of a MFHEX's hot and cold **flows** are entirely determined by the limiting temperature values $T^h_{out\_lim}$ and $T^c_{out\_lim}$, given the input parameters:

$$Q^h_{i\_lim} = \left(h^h_i\left(T^h_{i\_in}, P^h_i\right) - h^h_i\left(T^h_{out\_lim}, P^h_i\right)\right) \dot{m}^h_i, \;\; i \in [1..\, N^h] \tag{12}$$

$$Q^c_{j\_lim} = \left(h^c_j\left(T^c_{out\_lim}, P^c_j\right) - h^c_j\left(T^c_{j\_in}, P^c_j\right)\right) \dot{m}^c_j, \;\; j \in [1..\, N^c] \tag{13}$$

here and hereafter, mathematical notations like $h^h_i\left(T^h_i, P^h_i\right)$ or $h^c_j\left(T^c_j, P^c_j\right)$ imply the use of the equation of state corresponding to a working fluid of the specific flow.

Any MFHEX flow's real heat content must be larger than zero (because we believe that every flow inevitably exchanges heat with other flows) and less than or equal to the value of its limiting heat content:

$$0 < Q^h_i \leq Q^h_{i\_lim}, \;\; i \in [1..\, N^h] \tag{14}$$

$$0 < Q^c_j \leq Q^c_{j\_lim}, \;\; j \in [1..\, N^c] \tag{15}$$

The limiting heat content of the hot Q^H_{LIM} and cold Q^C_{LIM} ***bundles*** of a MFHEX (recall that a MFHEX's bundle is a set of either all the hot or all the cold flows) is the sum of the limiting heat content of the flows included in the bundle:

$$Q^H_{LIM} = \sum_{i}^{N^h} Q^h_{i\_lim} \tag{16}$$

Preprints.org (www.preprints.org) | NOT PEER-REVIEWED | Posted: 14 November 2025 doi:10.20944/preprints202511.1092.v1

$$Q^{C}_{LIM} = \sum_{j}^{N^{c}} Q^{c}_{j\_lim}$$

The smaller of the limiting heat contents $(Q^{H}_{LIM}, Q^{C}_{LIM})$ (16) of the bundles is the maximum quantity of heat Q_{LIM} that may be transferred between bundles (i.e., all hot flows with all cold flows):

$$Q_{LIM} = \min(Q^{H}_{lim}, Q^{C}_{lim}) \tag{17}$$

Let us designate as an "active bundle" MFHEX's bundle of N^{a} flows with a greater maximum heat content and a "passive bundle" (of N^{p} flows) with a lower maximum heat content. A bundle's "activity" or "passivity" is only based on its maximum heat content ratio, not on whether it is hot or cold.

The quantity of heat Q_{act} that is actually transferred between the flows of a MFHEX's bundles may be calculated as a certain fraction of Q_{max}, much as in the case of a two-flow HEX, when irreversible losses in the heat exchange process are taken into consideration:

$Q_{act} = \varepsilon \cdot Q_{LIM}, \varepsilon \in]0..1]$ (see eq. (2))

The total heat Q_{act} transferred in a MFHEX is removed from *all hot flows*:

$$Q_{act} = \sum_{i=1}^{N^{h}} Q^{h}_{i} \tag{18}$$

and distributes (disperses, scatters, divides) among *all cold flows*:

$$Q_{act} = \sum_{j=1}^{N^{c}} Q^{c}_{j} \tag{19}$$

Passive Bundle

First, let's consider the perfect heat transfer with no losses $\varepsilon = 1$. In this case, the amount of heat released (or received) by each of the N^{p} *passive* (with a lower maximum heat content) bundle's flows will obviously equal the *maximum* heat content of the flow (eq. (12) or (13)). Here, the outlet temperature of the flow is equal to its corresponding limiting temperature $T^{h}_{out\_lim}$ or $T^{c}_{out\_lim}$. The distribution of the total heat amount $Q_{act} = Q_{max}$ transferred between the bundle flows is then known:

Passive bundle	**Heat transfer in a MFHEX without losses: $\varepsilon = 1$**	
Hot	$\psi^{id}_{i} = \dfrac{Q^{h}_{i\_lim}}{Q_{LIM}}, \ i \in [1..\, N^{p} = N^{h}]$	(20)
Cold	$\psi^{id}_{j} = \dfrac{Q^{c}_{j\_lim}}{Q_{LIM}}, \ j \in [1..\, N^{p} = N^{c}]$	(21)

Now, we assume that the relationship (eq. (20) or (21)) that was calculated for the case of ideal heat exchange still *holds true* when there are irreversible losses in the heat exchanger: $\varepsilon < 1$ and $Q_{act} < Q_{LIM}$. Next, using the values of ψ^{id}_{i} or ψ^{id}_{j} the amount of heat released Q^{h}_{i} (or received Q^{c}_{j}) by a distinct flow of the bundle and the temperature of the flows at the outlet $T^{h}_{i\_out}$ (or $T^{c}_{j\_out}$), will be computed:

Passive bundle	**Heat transfer in a MFHEX with losses: $\varepsilon < 1$**	
Hot	$Q^{h}_{i} = Q_{act} \cdot \psi^{id}_{i}$,	(22)

	$h^h_{i\_out} = h^h_{i\_in} - \frac{Q^h_i}{\dot{m}^h_i}$, где $h^h_{i\_in} = h^h_i\left(T^h_{i\_in}, P^h_i\right) - invar.$ $s^h_{i\_out} = s^h_i\left(h^h_{i\_out}, P^h_i\right)$, $T^h_{i\_out} = T^h_i\left(h^h_{i\_out}, P^h_i\right), \qquad i \,\epsilon\, [1..\, N^p = \ N^h]$	
Cold	$Q^c_j = Q_{act} \cdot \psi^{id}_j$, $h^c_{j\_out} = h^c_{j\_in} + \frac{Q^c_j}{\dot{m}^c_j}$, где $h^c_{j\_in} = h^c_j\left(T^c_{j\_in}, P^c_j\right) - invar.$ $s^c_{j\_out} = s^c_j\left(h^c_{j\_out}, P^c_j\right)$, $T^c_{j\_out} = T^c_j\left(h^c_{j\_out}, P^c_j\right), \qquad j \,\epsilon\, [1..\ \ N^p = \ N^c]$	(23)

Active Bundle

By definition, the limiting heat content of the active bundle Q^H_{LIM} (or Q^C_{LIM}) *exceeds* the amount of heat Q_{act} actually transferred in a MFHEX. Consequently, the heat content Q_i of each of the N^a flows of the active bundle cannot simultaneously be equal to its limiting values, as in the case of a passive bundle. Specific values of Q_i (or their ratio) are not defined and depend on the conditions of heat exchange between flows, the thermophysical properties of the flow substance, phase state, mass flow rate, etc. Only the ranges of changes in the heat content of the flows are known with certainty: $0 < Q_i \leq Q_{i\_lim}$, subject to the condition $\sum Q_i = Q_{act}$.

Since thermodynamic calculations of heat transfer do not use either the heat transfer equations or the actual concepts of heat transfer coefficients and heat transfer surfaces, it is impossible to directly calculate either the ***specific*** values of Q^h_i (or Q^c_j) in eq. (18), (19), or the temperature of the active bundle flows at the outlet ports of a MFHEX. As a brute-force method in this case, a set of n_j values of allowable heat contents $Q_{i,j}$ from the range $0 < Q_{i,j} \leq Q_{i\_lim}$; $i\, \in [1..\, N^a], j \,\epsilon \left[1..n_j\right]$ can be set for each i^{th} flow of the active bundle. From these N^{ab} sets of $Q_{i,j}$, every potential combination of active bundle flows' heat content $(Q_{1,j},\ Q_{2,j},\ \ldots,\ Q_{N,j})$ that corresponds to the condition $\sum Q_i = Q_{act}$ can be obtained. Since the heat content and temperature of the passive bundle flows are already known by this moment (see eqs. (22), (23)), it becomes possible to calculate the *Tq*-diagrams for a MFHEX for all the sets $(Q_{1,j},\ Q_{2,j},\ \ldots,\ Q_{N,j})$ obtained. The results of the calculation are to be examined (sorted) in accordance with the given criteria. Such criteria might include one of the following: the minimum difference between the actual and limiting values of the flows' temperature at the MFHEX's outlet ports; the lowest possible irreversibility in the heat exchange processes between the flows (the minimum value of the rate of entropy production in an MFHEX); etc.

An Array of Feasible Heat Contents for an Individual Flow

It is technically more convenient to combine shares φ_i of the active bundle flows heat content (with in mind that the active bundle can be either a "hot" or a "cold" one) rather than their actual values Q_i:

$$\varphi_i = \frac{Q_i}{Q_{act}}, \qquad i \in [1..\, N^a];\ \sum\nolimits_i^{N^a} \varphi_i = 1. \qquad (24)$$

Let's set the minimum value of φ_i, the same for all flows in the bundle: φ_{min}. The maximum value of φ_{i_max} may vary from flow to flow, and its specific value is determined by restrictions (14),

Preprints.org (www.preprints.org) | NOT PEER-REVIEWED | Posted: 14 November 2025 doi:10.20944/preprints202511.1092.v1

(15) on the heat content of the flow. The ban on the zero heat content of the flow $Q_{i\_min} > 0$ (in fact, this is a ban on the "non-participation" of the flow in heat exchange) means that φ_{max} depends on the number of flows N in the bundle, since $Q_{i_{max}} = Q_{act} - \sum_{i=1}^{N^a-1} Q_{i\_min}$:

$$\varphi_{max} = 1 - \varphi_{min}(N^a - 1) \tag{25}$$

Taking into account the second restriction, which states that $Q_i \leq Q_{i\_lim}$, φ_{max} is contingent upon each flow specific parameters and is limited to the following value:

$$\varphi'_{i\_max} \leq \frac{Q_{i\_lim}}{Q_{act}} \tag{26}$$

The smaller of φ_{max} and φ'_{i_max} is chosen as the actual value, φ_{i_max}:

$$\varphi_{i\_max} = \min\left(\varphi_{max}, \varphi'_{i\_max}\right),\ \ i \in [1..\ N^a] \tag{27}$$

Thus, for every i^{th} flow of the active bundle (refer to eqs. (16), (17)), a vector $\varphi_i \in [\varphi_{min} .. \varphi_{i\_max}], i \in [1..\ N^a]$, can be assigned:

$$\begin{gathered}\varphi_{i,j} = \varphi_{min} + \frac{\varphi_{i\_max} - \varphi_{min}}{n_\varphi - 1}(j-1),\ \ i \in [1..\ N^a]\ \ \text{– bundle's flow index;} \\ j \in [1..n_\varphi] \text{ – vector's } \varphi_i \text{ element index;}\end{gathered} \tag{28}$$

In eq. (28) you can set the value n_φ the same for all flows. Then the increment in φ_i:

$$\Delta\varphi_i = \varphi_{i,j+1} - \varphi_{i,j} = \frac{\varphi_{i\_max} - \varphi_{min}}{n_\varphi - 1} \tag{29}$$

can vary from flow to flow. You can keep $\Delta\varphi$ the same for all flows, but then the vectors $\varphi_{i,j}$ will have different lengths:

$$n_{\varphi_i} = INT\left(\left(\varphi_{i\_max} - \varphi_{min}\right)/\Delta\varphi\right),\ \Delta\varphi - const;\ n_{\varphi_i} - var. \tag{30}$$

Both choices are equal and valid.

A set $\boldsymbol{A}$ is a useful way to express the collection of vectors $\varphi_{i,j}$ that are calculated for *each* active bundle 's *flow* $i \in [1..\ N^a]$:

$$\boldsymbol{A} = \left\{\begin{matrix}\left(\varphi_{1,1}, \varphi_{1,2}, \dots, \varphi_{1,n_{\varphi_1}}\right) \\ \left(\varphi_{2,1}, \varphi_{2,2}, \dots, \varphi_{2,n_{\varphi_2}}\right) \\ (--,--,\dots,--) \\ \left(\varphi_{N^a,1}, \varphi_{N^a,2}, \dots, \varphi_{N^a,n_{\varphi_{N^a}}}\right)\end{matrix}\right\} \tag{31}$$

The set $\boldsymbol{A}$ consists of N^a vectors $\varphi_{i,j}$ that are typically diverse in their length n_{φ_i}.

A Set of all Feasible Distributions of the MFHEX's Overall Heat Load Between the Flows

The set $\boldsymbol{A}$ will be used to produce a set of *all feasible* and physically consistent distributions of the thermal load Q_{act} between the flows of the active bundle: $Q_{act} = \sum Q_i = \sum Q_{act}\varphi_i$.

Let us construct a vector of length N^a such that every element φ_i, $i \in [1..\ N^a]$ corresponds to one of the elements of the vectors of set $\boldsymbol{A}$ that are iterated successively, say for example, $\left(\varphi_{1,1}, \varphi_{2,2}, \varphi_{3,1}, \dots, \varphi_{N^a,n_{\varphi_{N^a}}}\right)$. Such a vector fully characterizes one of the various distributions of the thermal load Q_{act} across all N^a flows of the active bundle if the total of all components of this vector equals *1* (see eq. requirement (24)).

In order to obtain a set $\boldsymbol{B}$ of all possible options for distributing the thermal load Q_{act} between the N^a flows, one must first find *all possible* combinations of elements of the vectors of set $\boldsymbol{A}$ with each other. The well-known combinatorics technique—the Cartesian product of a set with itself—will be used to achieve this:

$$\boldsymbol{B} = \begin{Bmatrix} (\varphi_{1,1}, \varphi_{2,1}, \dots, \varphi_{N^a,1}) \\ (\varphi_{1,1}, \varphi_{2,1}, \dots, \varphi_{N^a,2}) \\ (--,--,\dots,--) \\ (\varphi_{1,n_{\varphi_1}}, \varphi_{2,n_{\varphi_2}}, \dots, \varphi_{N^a,n_{\varphi_{N^a}}}) \end{Bmatrix} \times \begin{Bmatrix} (\varphi_{1,1}, \varphi_{2,1}, \dots, \varphi_{N^a,1}) \\ (\varphi_{1,1}, \varphi_{2,1}, \dots, \varphi_{N^a,2}) \\ (--,--,\dots,--) \\ (\varphi_{1,n_{\varphi_1}}, \varphi_{2,n_{\varphi_2}}, \dots, \varphi_{N^a,n_{\varphi_{N^a}}}) \end{Bmatrix} =$$

$$= \begin{Bmatrix} (\varphi_{1,1}, \varphi_{2,1}, \varphi_{3,1}, \dots, \varphi_{N^a,1}) \\ (\varphi_{1,1}, \varphi_{2,1}, \varphi_{3,1}, \dots, \varphi_{N^a,2}) \\ (\varphi_{1,1}, \varphi_{2,1}, \varphi_{3,1}, \dots, \varphi_{N^a,3}) \\ (--,--,--,\dots,--) \\ (\varphi_{1,n_{\varphi_1}}, \varphi_{2,n_{\varphi_2}},, \varphi_{3,n_{\varphi_3}} \dots, \varphi_{N^a,n_{\varphi_{N^a}}}) \end{Bmatrix} = \begin{Bmatrix} B_1 \\ B_2 \\ B_3 \\ \dots \\ B_{N_B} \end{Bmatrix} \quad (32)$$

Consequently, we are left with a set $\boldsymbol{B}$ made up of $N_{\boldsymbol{B}} > N_{\boldsymbol{A}}$ vectors, each of length N^a, which is equal to the number of flows in the active bundle. In general, the sum of the elements $\varphi_{i,j}$ of an arbitrary vector of the set $\boldsymbol{B}$ may differ from 1. By eliminating from the set $\boldsymbol{B}$ all the vectors for which the condition $\sum_{j=1}^{N^a} B_{i,j} = 1, i \in [1, N_{\boldsymbol{B}}]$ is false, we may reduce the set $\boldsymbol{B}$ to its subset $\boldsymbol{C}$:

$$\boldsymbol{C} = \begin{Bmatrix} C_1 \\ C_2 \\ C_3 \\ - \\ C_{N_C} \end{Bmatrix} = \begin{Bmatrix} (\varphi_{1,1}, \varphi_{2,1}, \varphi_{3,1}, \dots, \varphi_{N^a,1}) \\ (\varphi_{1,1}, \varphi_{2,1}, \varphi_{3,1}, \dots, \varphi_{N^a,2}) \\ (\varphi_{1,1}, \varphi_{2,1}, \varphi_{3,1}, \dots, \varphi_{N^a,3}) \\ (--,--,--,\dots,--) \\ (\varphi_{1,n_{\varphi_1}}, \varphi_{2,n_{\varphi_2}},, \varphi_{3,n_{\varphi_3}} \dots, \varphi_{N^a,n_{\varphi_{N^a}}}) \end{Bmatrix} \; \Bigg| \; \begin{Bmatrix} \sum_{j=1}^{N^a} C_{1,j} = 1 \\ \sum_{j=1}^{N^a} C_{2,j} = 1 \\ -------- \\ \sum_{j=1}^{N^a} C_{N_C,j} = 1 \end{Bmatrix} \quad (33)$$

Set $\boldsymbol{C}$ contains $N_{\boldsymbol{C}} < N_{\boldsymbol{B}}$ elements that represent vectors $(\varphi_{i,1}, \varphi_{i,2}, \dots, \varphi_{i,N^a}), i \in [1..N_{\boldsymbol{C}}]$ of all possible distributions of the thermal load Q_{act} between the flows of the active bundle (precisely to the magnitude of $\Delta\varphi_i$, see eq. (29)). Fulfillment of the condition $\sum_{j=1}^{N^a} C_{i,j} = 1, i \in [1..N_{\boldsymbol{C}}]$ means that each vector C_i will correspond to the heat balance condition for the flows of the active bundle (24): $\sum Q_i = \sum \varphi_i Q_{act} = Q_{act}$.

The transition from the heat content fractions $\varphi_{i,j}$ in the set $\boldsymbol{C}$ to the (T, h, s)—parameters of the active bundle flows at the exit from the MFHEX—is as follows:

Active bundle	**Heat transfer in a MFHEX with losses: $\varepsilon < 1$**	
Hot	$h^h_{i,j\_out} = h^h_{i\_in} - \dfrac{Q_{act} \cdot \varphi_{i,j}}{\dot{m}^h_i}$, $where\ h^h_{i\_in} = h^h_i(T^h_{i\_in}, P^h_i) - invar.$ $s^h_{i,j\_out} = s^h_i(h^h_{i,j\_out}, P^h_i)$, $\Delta S^h_{i,j} = (s^h_{i,j\_out} - s^h_{i\_in})\dot{m}^h_i < 0, where\ s^h_{i\_in} = s^h_i(T^h_{i\_in}, P^h_i) - invar.$ $T^h_{i,j\_out} = T^h_i(h^h_{i,j\_out}, P^h_i)$, $\Delta T^h_{i,j\_out} = T^h_{out\_lim} - T^h_{i,jout} < 0$, $where\ T^h_{out\_lim}$ see eq. (10)	(34)

$$i \in [1..\ N^h];\quad j \in [1..N_C]$$

Cold

$$h^c_{i,j\_out} = h^c_{i\_in} + \frac{Q_{act} \cdot \varphi_{i,j}}{\dot{m}^c_i},\ \ where\ h^c_{i\_in} = h^c_i\left(T^c_{i\_in}, P^c_i\right) - invar.$$

$$s^c_{i,j\_out} = s^c_i\left(h^c_{i,j\_out}, P^c_i\right),$$

$$\Delta S^c_{i,j} = \left(s^c_{i,j\_out} - s^c_{i\_in}\right)\dot{m}^c_i > 0, where\ s^c_{i\_in} = s^c_i\left(T^c_{i\_in}, P^c_i\right) - invar. \quad (35)$$

$$T^c_{i,j\_out} = T^c_i\left(h^c_{i,j\_out}, P^c_i\right),$$

$$\Delta T^c_{i,j\_out} = T^c_{out\_lim} - T^c_{i,jout} > 0,\ \ where\ \ T^c_{out\_lim}\ \text{ see eq. (11)}$$

$$i \in [1..\ N^c];\quad j \in [1..N_C]$$

The parameters h_{i,j_out} and T_{i,j_out} are directly employed in equations (34), (35) to compute the MFHEX's ***Tq***-diagrams, and the differences $\Delta T_{i,j}$ and $\Delta S_{i,j}$are used to first sort the set of potential solutions, which will be covered below.

By successively applying the relevant equations (34) (or (35)) to every element $\varphi_{i,j}$ in set ***C***, we can derive a set ***D*** of potential parameters for the active bundle flows at the MFHEX's exit:

$$\boldsymbol{D} = \begin{Bmatrix} D_1 \\ D_2 \\ D_3 \\ - \\ D_{N_D} \end{Bmatrix} = \begin{Bmatrix} \left((T,h,\Delta T,\Delta S)_{1,1\_out}, (T,h,\Delta T,\Delta S)_{1,2\_out}, \dots, (T,h,\Delta T,\Delta S)_{1,N^a\_out}\ \right) \\ \left((T,h,\Delta T,\Delta S)_{2,1\_out}, (T,h,\Delta T,\Delta S)_{2,2\_out}, \dots, (T,h,\Delta T,\Delta S)_{2,N^a\_out}\ \right) \\ \left((T,h,\Delta T,\Delta S)_{3,1\_out}, (T,h,\Delta T,\Delta S)_{3,2\_out}, \dots, (T,h,\Delta T,\Delta S)_{3,N^a\_out}\ \right) \\ ((----)-), (----), \dots, (----)) \\ \left((T,h,\Delta T,\Delta S)_{N_D,1\_out}, (T,h,\Delta T,\Delta S)_{N_D,2\_out}, \dots, (T,h,\Delta T,\Delta S)_{N_D,N^a\_out}\ \right) \end{Bmatrix} \quad (36)$$

Each array D_i of output parameters of the active bundle flows in the set (36) taken together with the set of invariable output parameters of the passive bundle flows (refer to eqs. (22) and (23)) specifies some operating mode of a MFHEX. This data is sufficient to calculate the ***Tq***-diagram of the mode.

By going successively from vector to vector in (36): D_1, D_2, …, D_D, ***Tq***-diagrams for every operational mode of MFHEX may be computed. After all the diagrams are analyzed further, only the most suitable diagram will be chosen based on performance evaluation criteria (see **Algorithm to compute the 2-flow heat exchanger's Tq-diagram**). This strategy has clear costs. It makes sense to first sort the MFHEX's operating modes that match the vectors D_i (36), based on the objective functions $F_{\Delta S\_j}$ or $F_{\Delta T_j}$ reported below. We will calculate ***Tq***-diagrams for a set of *sorted* vectors D_i up to the first operable diagram.

Objective Functions $\boldsymbol{F_{\Delta S\_j}}$ *or* $\boldsymbol{F_{\Delta T_j}}$ *to Rank the MFHEX Operational Modes*

According to the principles of thermodynamics, an ideal heat transfer process is the one that is reversible and generates either zero or very little entropy. Consequently, operating modes of heat exchangers with a smaller total change in the entropy of flows are thermodynamically more preferable because they mean lower losses during heat exchange. Now let's put down the objective function $F_{\Delta S\_j} \to min$ related to the MFHEX's change in flows entropy:

$$F_{\Delta S\_j} = \sum\nolimits_{i=1}^{N^h} \left(S^h_{i\_out} - S^h_{i\_in}\right)\dot{m}^h_i + \sum\nolimits_{i=1}^{N^c} \left(S^c_{i\_out} - S^c_{i\_in}\right)\dot{m}^c_i \to min, \qquad j \in [1..N_D] \quad (37)$$

For every element-vector D_i in the set (36), $F_{\Delta S}$ is calculated and then all the elements of D_i are sorted using the rising function $F_{\Delta S}(D_i)$:

Preprints.org (www.preprints.org) | NOT PEER-REVIEWED | Posted: 14 November 2025 doi:10.20944/preprints202511.1092.v1

$$\boldsymbol{D}_{sorted\_\Delta S} = \begin{Bmatrix} D_i \\ D_j \\ D_k \\ - \\ D_l \end{Bmatrix} = \begin{Bmatrix} F_{\Delta S}(D_i) < F_{\Delta S}(D_j) \\ F_{\Delta S}(D_j) < F_{\Delta S}(D_k) \\ F_{\Delta S}(D_k) < \quad - - \\ - - \quad < \quad - - \\ - - \quad < F_{\Delta S}(D_l) \end{Bmatrix} \tag{38}$$

The minimal difference between the actual temperature values T_{i,j_out} (see eqs. (34) –(36)) of the active bundle flows at the MFHEX's outlet and their upper limit values T_{out_lim} (see eqs. (10) and (11)) might serve as an alternate criterion for the heat exchanger's efficiency:

$$F_{\Delta T_j} = \Delta\bar{T}_j + \Delta\bar{\bar{T}}_j \to min, \qquad j \in [1..N_D]$$

$$\Delta\bar{T}_j = \frac{1}{N^a}\sum_{i=1}^{N^a} \Delta T_{i,j}, \qquad i \epsilon [1..\ N^a];\ \ j \in [1..N_D]$$

$$\Delta\bar{\bar{T}}_j = \frac{1}{N^a}\sum_{i=1}^{N^a} \left|\Delta\bar{T}_j - \Delta T_{i,j}\right|, \qquad i \epsilon [1..\ N^a];\ \ j \in [1..N_D] \tag{39}$$

$$where,$$

$$\Delta T_{i,j} = \left|T^h_{out\_lim} - T^h_{i,j_{out}}\right|, \quad \text{hot bundle} \quad \text{– active, see (34)}$$

$$\Delta T_{i,j} = \left|T^c_{out\_lim} - T^c_{i,j_{out}}\right|, \quad \text{cold bundle} \quad \text{– active, see (35)}$$

Since the outlet temperatures of the passive bundle flows (see eqs. (22) and (23)) do not change throughout the computations, the objective function (39) can be applied only to the outlet temperatures of the active bundle flows.

The minimum value of the function $F_{\Delta T_j} = \Delta\bar{T}_j + \Delta\bar{\bar{T}}_j$ implies that the outlet temperatures of the active bundle flows have values as close as possible to their limiting value: $\left(T_{i_{out}} \to T_{out\_lim}\right) \Rightarrow (\Delta\bar{T} \to min)$, with the minimum possible "scatter" of their values around $\Delta\bar{T}$: $(\Delta T_i \to \Delta\bar{T}) \Rightarrow (\Delta\bar{\bar{T}} \to min)$.

As in the case of $F_{\Delta S}$, $F_{\Delta T}$ is computed for every vector element D_i in the set (36) and the elements D_i are then sorted using the increasing function $F_{\Delta T}(D_i)$:

$$\boldsymbol{D}_{sorted\_\Delta T} = \begin{Bmatrix} D_i \\ D_j \\ D_k \\ - \\ D_l \end{Bmatrix} = \begin{Bmatrix} F_{\Delta T}(D_i) < F_{\Delta T}(D_j) \\ F_{\Delta T}(D_j) < F_{\Delta T}(D_k) \\ F_{\Delta T}(D_k) < \quad - - \\ - - \quad < \quad - - \\ - - \quad < F_{\Delta T}(D_l) \end{Bmatrix} \tag{40}$$

It should be emphasized that, in contrast to the situation of minimizing the function $F_{\Delta S}$, the objective function $F_{\Delta T}$ may be computed simultaneously for *all flows* of the active bundle, for flows that have been individually chosen, or even for *a single flow* if necessary.

Algorithm to Compute the Multi-Flow Heat Exchanger's Tq-Diagram

Just as in the case of 2-flow HEX, the MFHEX is divided into n sections along its length in order to calculate the Tq-diagram:

$$n = INT\left(\frac{\max\limits_{0 \le i \le N^h} T^h_{i\_in} - \min\limits_{0 \le j \le N^c} T^c_{j\_in}}{\Delta T}\right), \tag{41}$$

where ΔT is the flows temperature increment (decrement) within one section. The specific value of ΔT, let's say, $10\ K$ is chosen subjectively, based on the consideration that the nature of the change in the flows' thermodynamic properties within each individual section is about to be linear.

At this point, the outlet parameters of the passive bundle flows have already been calculated and are assumed to be unchanged for all operating modes of the MFHEX (see (22) and (23)). The set of potential outlet parameters of the active bundle flows is also calculated and sorted (see eqs. (38) or (40)) in accordance with the selected objective function. Let us recall that any of the MFHEX's modes of operation is completely determined by a set of outlet parameters of the active bundle flows (grouped in D_i arrays of the set $\boldsymbol{D_{sorted\_\Delta S}}$ or $\boldsymbol{D_{sorted\_\Delta T}}$) and a set of invariable outlet parameters of the passive bundle flows.

To find out if a certain MFHEX operating mode has an operable Tq-diagram, you need to figure out the distribution of the flow enthalpies h_k and the corresponding temperatures T_k (where k is the flow cross-section) for the outlet parameters of the flows that go with that mode:

$$\begin{aligned} &h^h_{i,k} = h^h_{i\_in} - \frac{h^h_{i_{in}} - h^h_{i_{out}}}{n} \cdot (n-k), \\ &T^h_{i,k} = T^h_i\left(h^h_{i,k}, P^h\right), \qquad i \in [1..\ N^h],\quad k \in [0..n];\ ; \end{aligned} \tag{42}$$

$$\begin{aligned} &h^c_{j,k} = h^c_{j\_in} + \frac{h^c_{j\_out} - h^c_{j\_in}}{n} \cdot k, \\ &T^c_{j,k} = T^c_j\left(h^c_{j,k}, P^c\right), \qquad j \in [1..\ N^c],\quad k \in [0..n];\ ; \end{aligned} \tag{43}$$

For all $i-j$ pairs of i-hot ($i \in [1..\ N^h]$) and j-cold ($j \in [1..\ N^c]$) the MFHEX flows, the temperature differences in all $k \in [0..n]$ sections are determined: $\Delta T_{i,j,k}$. Next, the minimal temperature difference $\Delta T_{i,j\_min}$ for each $i-j$ pair, and the heat exchanger as a whole, ΔT_{MFHEX_min}, is chosen:

$$\begin{aligned} &\Delta T_{i,j,k} = T^h_{i,k} - T^c_{j,k}, \qquad i \in [1..\ N^h],\quad j \in [1..\ N^c],\quad k \in [0..n]; \\ &\Delta T_{i,j\_min} = min\left(\Delta T_{i,j,k}\right); \qquad i \in [1..\ N^h],\quad j \in [1..\ N^c],\quad k \in [0..n]; \\ &\Delta T_{MFHEX\_min} = min\left(\Delta T_{i,j\_min}\right); \qquad i \in [1..\ N^h],\quad j \in [1..\ N^c]; \end{aligned} \tag{44}$$

The MFHEX operating mode and the Tq-diagram that goes with it are said to be operational when the following condition is met:

$$\Delta T_{MFHEX\_min} \ge \Delta T_{min}, \tag{45}$$

Here, ΔT_{min} is the minimum temperature difference that is allowed between MFHEX flows.

If condition (45) is not met, then calculation (42)-(45) is to be repeated for the next operating mode of the MFHEX, the next vector-array Di of set (38) or (40).

If condition (45) is not satisfied for any of the elements of the set $\boldsymbol{D_{sorted\_\Delta S}}$ (eq. (38)) or $\boldsymbol{D_{sorted\_\Delta T}}$ (eq. (40)), then this means that, under given initial conditions, the amount of heat Q_{act} (see eqs. (16)-(18)) cannot be transferred from all hot to all cold flows under any heat transfer

Preprints.org (www.preprints.org) | NOT PEER-REVIEWED | Posted: 14 November 2025 doi:10.20944/preprints202511.1092.v1

conditions. In order to get a feasible Tq-diagram, it is necessary to decrease Q_{act} by lowering the heat transfer efficiency coefficient ε (eq. (2)).

4. Validation of Calculation Results

The presented algorithm for a MFHX Tq-diagram calculation has been translated into computer code for Python v. 3.5. The code exploits a set of numerical computer subroutines developed by the National Institute of Standards and Technology (NIST) [2] to calculate thermodynamic and transport properties for various fluids and mixtures.

We carried out calculations of Tq-diagrams of 2- and 3-flow HEXs for a number of values of the minimum allowable temperature differences ΔT_{min} between flows. The acquired data was validated by comparing it to the results of calculations of similar heat exchangers in the Aspen HYSYS 12.1 program[3].

4.1. 2-Flow HEX

The initial data for cold and hot flows in a 2-flow HEX[4] is presented in *Table 1*. We want to point out that in order to compute the Tq-diagram, one also needs to define the lowest allowable temperature difference ΔT_{min} between the flows (see eqs. (9) and (45)) and the error $\delta\varepsilon$ in determining the HEX's coefficient of efficiency (see (2)). The following computation results were all acquired with an error of $\delta\varepsilon = 0.0001$.

We consider the Tq-diagram of the heat exchanger to be "operable" if the minimum temperature difference between the flows is greater than or equal to the specified value ΔT_{min}. The calculation and analysis of "operable" diagrams occurs in the range of the HEX's efficiency $\varepsilon \in [0.01, 1.0]$ using the golden section method until the condition is met: $(\varepsilon_{max} - \varepsilon_{min}) \leq \delta\varepsilon$. If this condition is met, the Tq-diagram for ε_{max} will be "inoperable" (the minimum temperature difference between the flows is less than the specified ΔT_{min}), and for ε_{min} it will be "operable".

The following calculations are presented in *Table 2*, depending on the specified minimum allowable temperature difference ΔT_{min} between the flows:

- the HEX's efficiency: $\varepsilon' = Q_{act}/Q_{act}\,(\Delta T_{min} = 0)$;
- the amount of heat Q_{act} transferred in the HEX;
- the temperature differences: at the HEX hot end $(T_{hot\_in} - T_{cold\_out})$;
- cold end $(T_{hot\_out} - T_{cold\_in})$;
- the minimum calculated temperature difference between the flows inside the HEX.

Table 2. Results of the 2-flow HEX calculation based on ΔT_{min} ($\delta\varepsilon = 0.0001$; $\Delta T_{as} = 5.0$, K).

ΔT_{min}	ε'	Q_{act}	$T_{hot} - T_{cold}$		
			hot port	cold port	internal, min
K		W		K	
0.0	1.00	66992.8	31.3	14.9	0.0002
2.0	0.98	65324.1	32.9	18.8	2.0009
3.0	0.96	64490.4	33.8	20.6	3.0007
5.0	0.94	62820.6	35.5	24.4	5.0027
8.0	0.88	58627.4	39.7	33.3	8.0000

[2] The NIST REFPROP program applies the most appropriate thermodynamic models for various fluids and mixtures under the umbrella term "the default recommended equation of state," which is delivered as a collection of computer procedures assembled into a single DLL.

[3] AspenTech HYSYS AspenONE 12.1 License for Order # 130050AK2O2; National Research and Development Institute for Cryogenic and Isotopic Technologies, Rm. Valcea, Romania.

[4] The initial data for this HEX is taken from a practically implemented methane liquefier flowsheet.

Preprints.org (www.preprints.org) | NOT PEER-REVIEWED | Posted: 14 November 2025 doi:10.20944/preprints202511.1092.v1

In the course of the computation, the operating modes were sorted and ranked using the objective function $F_{\Delta S\_j}$ (eq. (37). The computation results for the objective functions $F_{\Delta S\_j}$ (eq. (37)) and $F_{\Delta T_j}$ (eq. (39)) coincide in the case of the 2-flow HEX. *Figure 1C* and *Figure 3* provide a graph of the computed Tq-diagram of the 2-flow HEX in the scenario when ΔT_{min} = *5 K*.

The results of calculating a similar 2-flow HEX in the AspenTech HYSYS AspenONE 12.1 program are presented in *Table 3*.

Table 3. Results of the 2-flow HEX calculation in the HYSYS AspenONE 12.1 program.

$T_{hot} - T_{cold}$			Q_{act}	ε'
hot port	**cold port**	**internal, min**		
	K		W	
30.0	13.9	-2.9	66820.0	--
33.0	20.5	0.009	63880.0	1
35.0	24.7	2.0	61920.0	0.97
36.0	26.7	3.0	60940.0	0.95
38.0	30.6	5.0	58980.0	0.92

To calculate the Tq-diagram of the HEX, AspenTech allows you to set any values of the temperature difference between the flows at either the hot or cold ends of the HEX (see [7]). Apparently, the program does not analyze the limiting heat content of the flows and overlooks the possibility of the objective existence of a minimum temperature difference between the flows at one of the HEX's ends, under which one can't go down.

A user manually goes through the possible values of ΔT at either the hot or cold end of the HEX until he receives an operable Tq-diagram with the required value of the minimum temperature difference between the flows.

A satisfactory correlation is observed between the values of the HEX's efficiency ε' and the quantity of heat Q_{act} that is actually transferred in the HEX with a change in given ΔT_{min} in both calculations (see *Table 2* and *Table 3*). The values of ε' and Q_{act} computed by the reported program and HYSYS showed a relative difference of (1-2), %, and (4.6–6.1), %, respectively.

At the same time, the discrepancies between the corresponding values of the end temperature differences ($T_{hot} - T_{cold}$) with changes in ΔT_{min} are noticeably greater and amounted to: for the *hot end* (5.4–7.0), %, and for the *cold end* (25.4–37.6), % (see *Figure 2*). Reducing the temperature step along the flow by increasing the number of nodes n (eq. (41)) on the flow computational grid did not improve that situation.

Preprints.org (www.preprints.org) | NOT PEER-REVIEWED | Posted: 14 November 2025 doi:10.20944/preprints202511.1092.v1

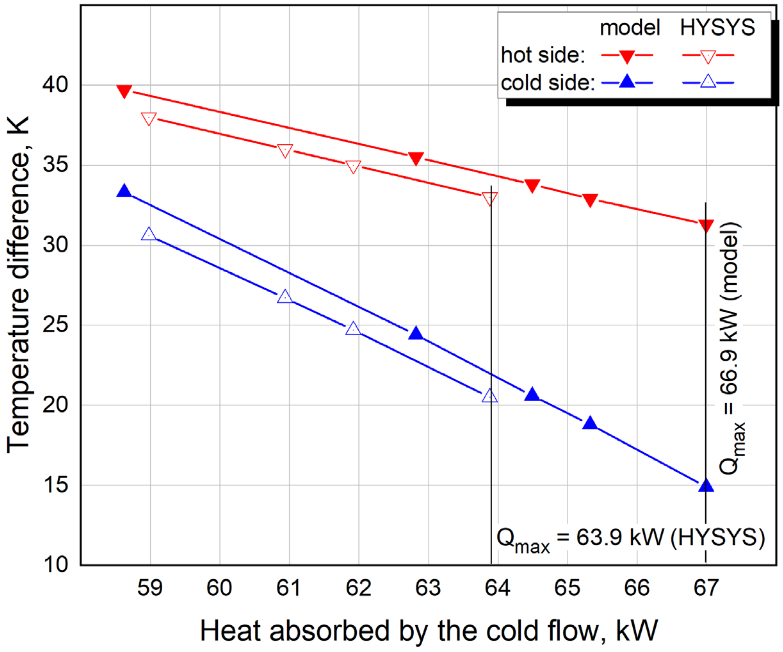

Figure 2. Temperature difference at the 2-flow HEX's ends: as determined by the computations shown in Table 2 and Table 3.

Figure 3 compares the Tq-diagrams of the considered 2-flow HEX, calculated in our program and in HYSYS for ΔT_{min} = 5 K. As can be seen from the temperature curves, the HEX's cold flow does not change its phase state, and both calculation programs show negligible differences in the distribution and range of temperature changes throughout the length of the cold flow.

At the same time, the hot flow is cooled from the state of superheated vapor to the subcooled liquid, and the distribution of temperatures in the flow, calculated by the programs, is significantly different. The divergence of curves occurs in the zones of transition from the vapor into the two-phase state. We believe it is unlikely that this may be due to the specifics of the Tq-diagram calculation algorithms used by the programs. Rather, it is the thermodynamic models used to calculate flow properties.

 doi:10.20944/preprints202511.1092.v1

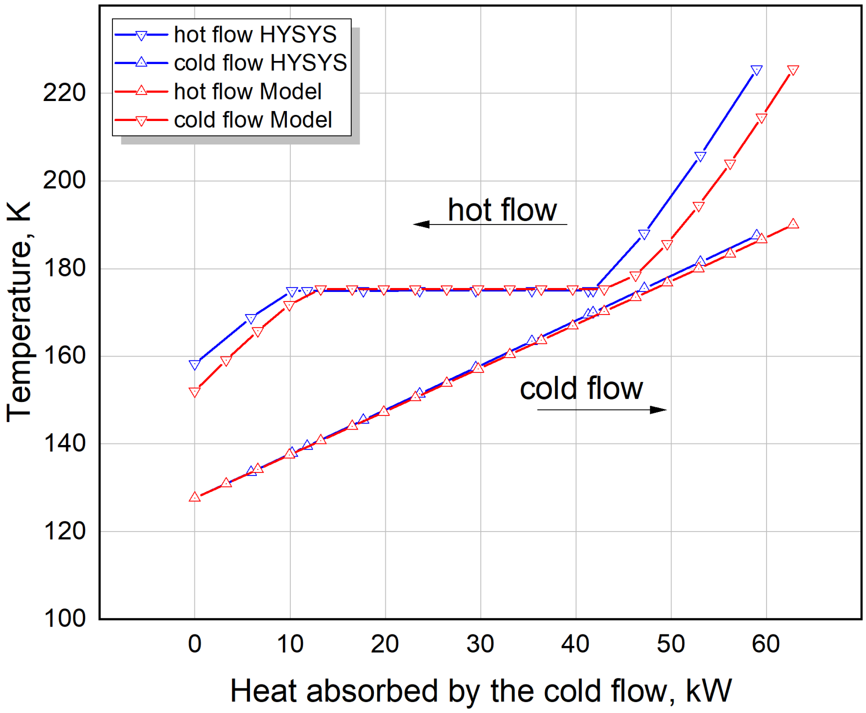

Figure 3. Comparison of Tq-diagrams of 2-flow HEX for $\Delta T_{min} = 5\ K$: calculation using the suggested model and HYSYS AspenONE 12.1.

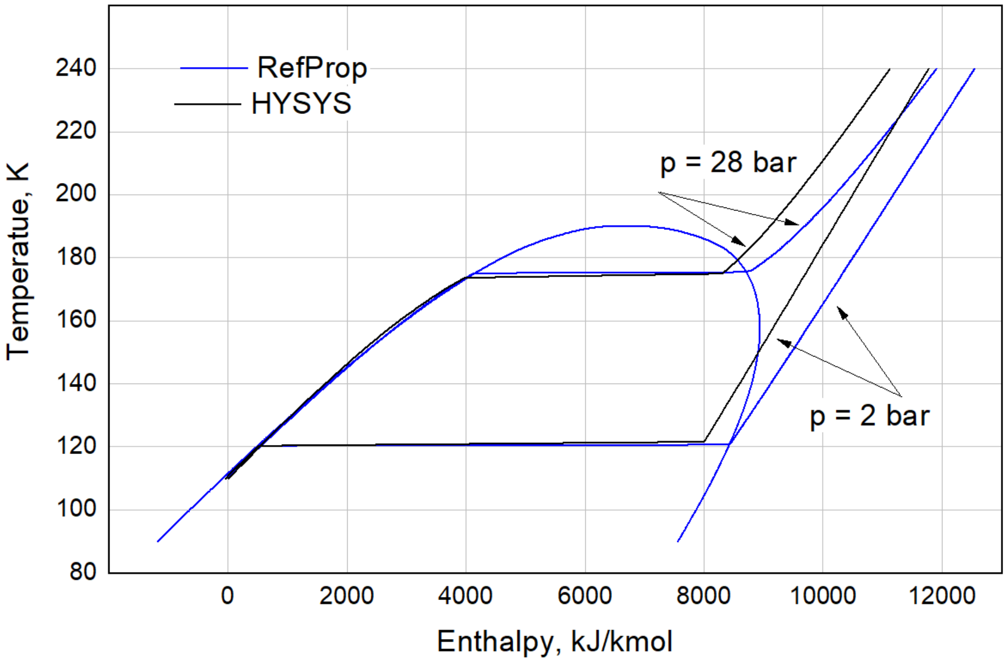

Figure 4. T-h diagram of the CH_4 - N_2 - O_2 mixture, where the composition matches that of the hot flow in the HEX (see Table 1).

To back up our assumption, *Figure 4* shows the *T-h* diagram of state plotted for the HEX's hot flow fluid (see *Table 1*). The 2-phase envelope and 2 isobars in blue are calculated with the default equation of state of REFPROP 10.0 [6]. Another 2 isobars in black are calculated with the Peng-Robinson thermodynamic model from AspenTech HYSYS AspenONE 12.1 [7]. It is clear that the isobars that were calculated using those models behave differently in the area of superheated vapor and in the two-phase envelope close to the fluid dew curve. Since analyzing the causes of such a disparity is beyond the purview of this study, we will only be able to conclude that the reported *Tq*-diagram calculation technique is unrelated to the reasons for certain discrepancies in the test calculations of that 2-flow HEX.

4.2. 3-Flow MHEX

An analysis was done on a 3-flow MFHEX[5], where two cold flows and one hot flow share the heat. *Table 4* contains the initial/input data needed to calculate the qT-diagram of this 3-flow MFHEX. Similar to the 2-flow HEX previously discussed, setting the minimum allowable temperature difference between the flows ΔT_{min} (refer to (9) and (45)) and the error in determining the MFHEX coefficient of efficiency $\delta\varepsilon$ (refer to (2)) are also required in order to calculate the qT-diagram of a MFHEX. The following computation results were obtained for $\varepsilon \in [0.01, 1]$ with a relative error of $\delta\varepsilon$ = 0.0001. The value of the temperature change along one section of the MFHEX: $\Delta T_{as} = T_{i+1} - T_i$ (refer to (7) and (8)) was taken to be *10* K, which corresponded to the division of the MFHEX into n = 19 sections.

Table 4. Initial data for calculating the Tq-diagram of the 3-flow MFHEX.

Flow		Working fluid		MFHEX flows inlet parameters		
type	index	component name	composition mol/mol	temperature K	pressure bar	mass rate kg/h
Hot	1	N_2	78.11	303.0	38.80	3292.0
		O_2	20.96			
		Ar	0.93			
Cold	1	N_2	62.21	104.8	1.50	1950.0
		O_2	36.18			
		Ar	1.61			
	2	N_2	1.0	160.0	1.50	1091.0

The results of the calculations of the 3-flow MFHEX using the algorithm we propose are presented in *Table 5*. The value of the minimum permissible temperature difference $\Delta T_{min} \in [0.0, 8.0], K$ between the MFHEX hot and each of the cold flows (shown in bold italics in *Table 5*) is an independently specified parameter in the calculations.

The following computed parameters of the MFHEX and its flows are shown in *Table 5* (subscripts hot, cold_1, and cold_2 denote hot and cold flows, respectively; numerals "1" and "2" correspond to *Table 4*'s cold flow indexes):

- the MFHEX's efficiency: $\varepsilon' = Q_{act}/Q_{act}\,(\Delta T_{min} = 0)$;
- the amount of heat Q_{act} transferred in the MFHEX;
- the salient temperature differences between the hot and cold flows $(T_{hot} - T_{cold\_1})$ and $(T_{hot} - T_{cold\_2})$: at the MFHEX's hot and cold port; minimum, maximum and average values inside the MFHEX.

In the course of the computation, the operating modes were sorted and ranked using the objective function $F_{\Delta T_j}$ (eq. (39)). The computation results for the objective functions $F_{\Delta S\_j}$ (eq. (37)) and $F_{\Delta T_j}$ (eq. (39)) coincide in the considered case of the 3-flow MFHEX.

AspenTech HYSYS AspenONE 12.1 [7] was used to model a similar 3-flow MFHEX in order to assess the adequacy of the data in *Table 5*. Peng-Robinson EOS was used as the program property package to calculate the thermodynamic and thermal properties of the MFHEX flows' working fluids.

Table 5. Results of the 3-flow MFHEX (see Table 4) calculation based on ΔT_{min} ($\delta\varepsilon$ = 0.0001; ΔT_{as} =10.0, K); objective function $F_{\Delta T\_j}$, (39).

[5] The initial data for this MFHEX is taken from a practically implemented ASU flowsheet.

ΔT_{min}	ε'	Q_{act}	$T_{hot} - T_{cold\_2}$			$T_{hot} - T_{cold\_1}$		
			cold port	hot port	internal, min/max/avr	cold port	hot port	internal, min/max/avr
K		kW			K			
0.0	1.00	147.069	5.03	4.12	0.001/5.03/1.67	60.23	5.73	5.73/60.23/30.28
2.0	0.98	144.965	6.55	6.11	2.00/6.55/3.60	61.75	8.50	8.50/61.75/32.59
3.0	0.97	143.908	7.31	7.11	3.01/7.31/4.57	62.51	9.89	9.89/62.51/33.76
5.0	0.96	141.781	8.96	9.12	5.00/9.12/6.53	64.16	12.69	12.69/64.16/36.11
8.0	0.94	138.547	11.52	12.18	8.00/12.18/9.52	66.72	16.95	16.95/66.72/39.69

In accordance with the AspenONE approach to calculating MFHEXs, the following temperature differences were specified between the hot flow inlet and the cold flow's outlet temperatures: $\Delta T_1 = (T_{hot\_in} - T_{cold\_1\_out})$ and $\Delta T_2 = (T_{hot\_in} - T_{cold\_2\_out})$. Both ΔT_1 and ΔT_2 were given as independent parameters in addition to the input data from *Table 4*. In this way, AspenONE's method differs dramatically from our method, where ΔT_{min} is the independent input parameter and ΔT_1 and ΔT_2 are both calculated along with other parameters.

Our plan was to use AspenONE to compute the MFHEX for every set of ΔT_1 and ΔT_2 values in *Table 5*. The results of those computations are shown in *Table 6*, which uses the same parameters designations as those in *Table 5*. Only the first row of *Table 6*, the MFHEX idealized operating mode with $\Delta T_{min} \to 0$, was obtained by manually varied values of ΔT_1 and ΔT_2 with accuracy of *1* K (those values have no match in *Table 5*).

While exploring the AspenONE model for an idealized operating mode, we discovered that the values $\Delta T_1 = 4.0\,K$ and $\Delta T_2 = 3.0\,K$ (refer to *Table 6*) match to the MFHEX limit of the lowest temperature difference between the hot flow and cold flow #2, which is $\Delta T_{min} = 0.1$, *K*. A further decrease in one of the parameters ΔT_1 or ΔT_2 led to the fact that in one of the internal sections of the MFHEX, the temperature of the cold flow 2 exceeded the temperature of the hot flow. Note that AspenONE designated the qT-diagrams of such modes as operational. Probably, the program evaluates the performance of the diagram not by comparing the temperatures of the flows in the calculated cross-sections of the MFHEX but by some other considerations.

To show this, *Figure 5* presents the qT-diagram that was calculated in the AspenONE 12.1 program for $\Delta T_1 = 2.0\,K$ and $\Delta T_2 = 3.0\,K$. It shows the relationship between the flow temperature and the amount of heat transferred in the way that the program shows it graphically. AspenONE marks this qT-diagram as "*working*". We have rebuilt this qT-diagram in *Figure 6* as the change in flow temperatures in the corresponding *10* cross sections of the heat exchanger, into which the AspenONE program divided it during the calculation process. With this interpretation of the diagram, it is clear that the temperature curves of the hot flow and cold flow 2 intersect.

Table 6. Results of the 3-flow MFHEX calculation (see Table 4) in the HYSYS AspenONE 12.1 program: the temperature difference at the MFHEX hot port (Thot – Tcold [1]) and (Thot – Tcold[2]) are given.

ΔT_{min}	ε'	Q_{act}	$T_{hot} - T_{cold\_2}$			$T_{hot} - T_{cold\_1}$		
			cold port	hot port	internal, min/max/avr	cold port	hot port	internal, min/max/avr
K		kW			K			
0.10	1.0	145.300	5.70	***3.00***	0.1/5.7/1.75	60.90	***4.00***	4.0/60.9/29.64
1.31	0.99	144.026	6.68	***4.12***	1.31/6.68/2.88	61.88	***5.73***	5.73/61.88/31.09
3.34	0.98	141.925	8.32	***6.11***	3.34/8.32/4.83	63.52	***8.50***	8.5/63.52/33.43
4.35	0.97	140.871	9.15	***7.11***	4.35/9.15/5.81	64.35	***9.89***	9.89/64.35/34.61
6.39	0.95	138.750	10.84	***9.12***	6.39/10.84/7.78	66.04	***12.69***	12.69/88.04/36.99
9.51	0.93	135.524	13.44	***12.18***	9.51/13.44/10.79	68.64	***16.95***	16.95/68.64/40.61

Since our main task is solely to check the adequacy of the calculation results using our algorithm, we will not go into an analysis of how AspenONE interprets the calculation results but will limit ourselves to comparing the calculation results in *Table 5* and *Table 6*.

Both calculations (*Table 5* and *Table 6*) show a satisfactory agreement between the values of the amount of heat actually transferred Q_{act}, the heat efficiency ε', and ΔT_{min} with changes in ΔT_1 and ΔT_2. The relative difference in the calculated Q_{act} values does not exceed 2.2%, with an average value of 2.1%. In the case of ε', the relative maximum/average calculation errors were 1.0/0.6%. The minimum temperature difference in the heat exchanger between hot and cold flows is within the limits $\Delta T_{min} \in [1.3, 9.5], K$. In this case, the average absolute calculation error of ΔT_{min} was 1.4 K, and the relative error was 27.2%.

Reducing the temperature step along the flow by increasing the number of nodes n (eq. (41)) on the flow computational grid did not enhance the results.

Figure 7 displays the qT-diagrams of the 3-flow MFHEX calculated in our program with the given $\Delta T_{min} = 5.0$ K (see *Table 5*) and the corresponding mode in AspenONE using $\Delta T_1 = 12.69\ K$ and $\Delta T_2 = 9.12\ K$ (see *Table 6*). Satisfactory agreement between the *T(q)* curves' runs suggests that the computation of the heat and temperature distribution in the flow over the heat exchanger's length was accurate.

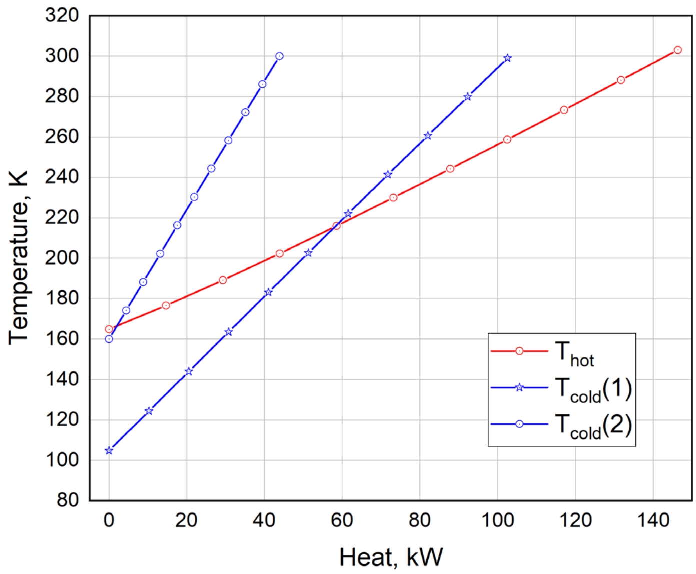

Figure 5. The 3-flow MFHEX flows' temperature with the heat transferred: simulated in the HYSYS AspenONE 12.1 program with given temperature difference at the MFHEX's hot side: ΔT_1 = 2.0, K; ΔT_2 = 3.0, K.

Figure 7 depicts the qT-diagram of the 3-flow HEX in the AspenONE way, where the flow temperatures depend on the heat transferred. This is a traditional representation of qT-diagrams that works perfectly for 2-flow heat exchangers, where the relation between the temperatures of both flows and the amount of heat transferred is clear and unambiguous. However, as seen in *Figure 5* and *Figure 6*, this method of displaying the qT-diagram for a multi-flow heat exchanger, however, tends to obscure the true relation between the temperatures of the flows. The qT-diagram on *Figure 5* looks like an operable one (and the AspenONE marks it as operable), while as it can be seen from *Figure 6*, the hot- and cold-2 temperature curves intersect. The relationship between the points on the temperature curves of the MFHEX flows is not readily apparent with this rendering of the qT-diagram, and more manipulations are necessary to look for it. It makes sense to link the temperature and the quantity of heat transferred indirectly, based on the MFHEX's cross-section, as seen in *Figure 8*, rather than directly, as in *Figure 7*. This kind of qT-diagram gives temperatures and heat fluxes along each section of a MFHEX, which is crucial information for the heat transfer analysis that follows the thermodynamic calculations. A snapshot of a graphical output window displaying the results of

Preprints.org (www.preprints.org) | NOT PEER-REVIEWED | Posted: 14 November 2025 doi:10.20944/preprints202511.1092.v1

qT-diagram calculations of the 3-flow MFHEX's (*Table 4*) operating mode with ΔT_{min} = 5.0 K, is shown in *Figure 9*.

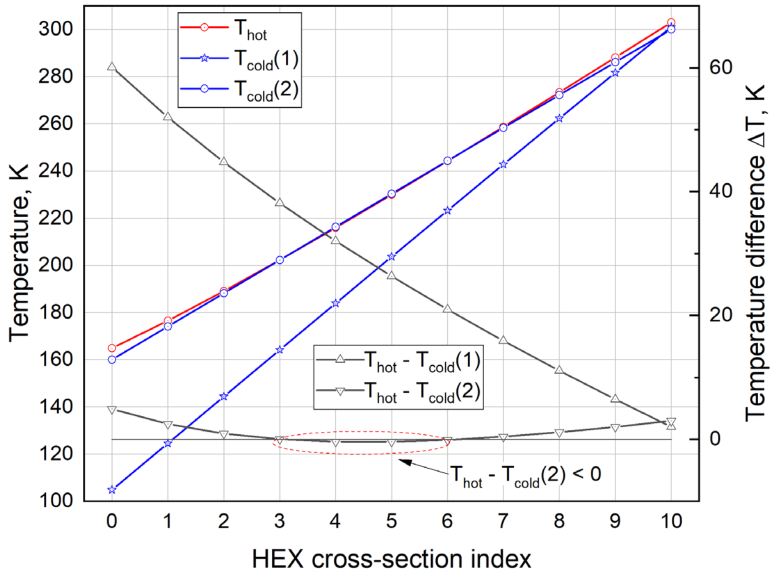

Figure 6. *The* 3-flow *MFHEX flows' temperature with the cross-sectional indexes: simulated* in the HYSYS AspenONE 12.1 program *with* given temperature difference at the MFHEX's hot side: ΔT_1 = 2.0, K; ΔT_2 = 3.0, K.

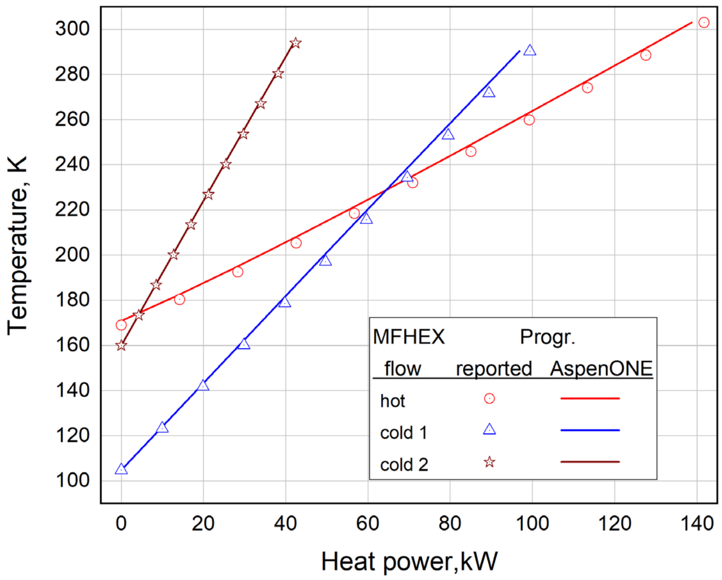

Figure 7. Comparison of the 3-flow MFHEX flows' temperature with the heat transferred: calculated in the program reported with ΔT_1 = 5, K, and simulated in the HYSYS AspenONE 12.1 program with ΔT_1 = 12.69, K; ΔT_2 = 9.12, K.

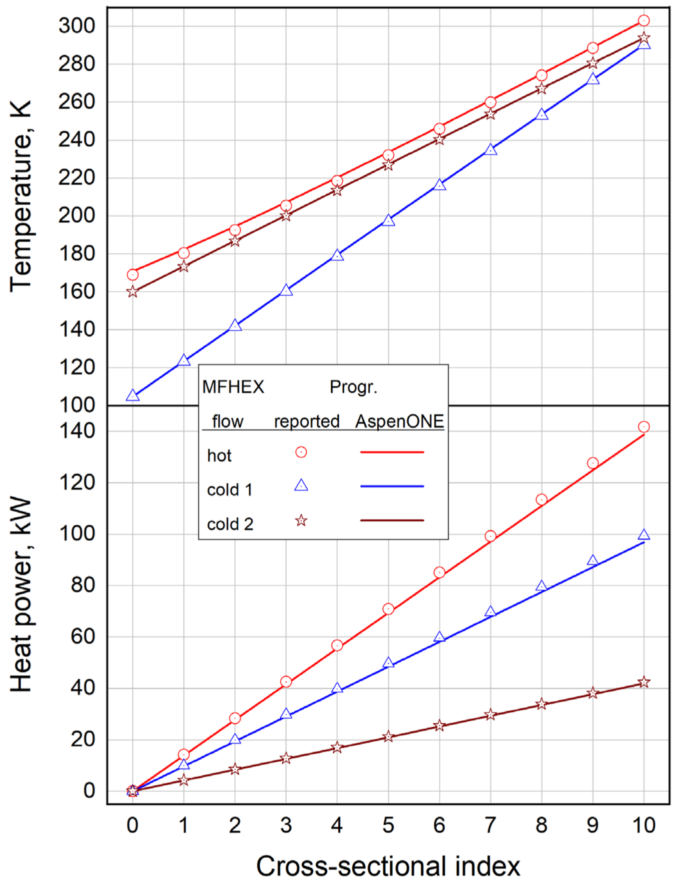

Figure 8. Comparison of the 3-flow MFHEX flows' temperature with the cross-sectional indexes: calculated in the program reported with $\Delta T_1 = 5$, K, and simulated in the HYSYS AspenONE 12.1 program with $\Delta T_1 = 12.69$, K; $\Delta T_2 = 9.12$, K.

5. Conclusions

1. A method for finding heat exchangers' operable qT-diagrams is proposed. The process entails calculating the maximum heat that can be transferred through the heat exchanger, examining the various ways that this heat could be distributed among all of the heat exchanger's flows, and then calculating qT-diagrams for each of these heat-spreading strategies, which are subsequently ranked and examined.
2. This method is general in that it can compute 2-flow HEXs as well as HEXs with an arbitrary number of hot and cold flows.
3. We made sure that the proposed method worked by comparing the results of calculations of qT-diagrams to the results of calculations of similar HEXs in the AspenONE HYSYS program.
4. A new representation of the qT-diagram for multi-flow heat exchangers as a pair of complementary diagrams, in which the cross-sectional index of the apparatus is used as the independent variable, has been proposed. The first one displays the temperature distribution of the flows, and the second one displays the quantity of heat transferred between the flows taken in pairs. Unlike the traditional approach, this representation allows unambiguous identification of temperature pairs of the flows at each cross-section and eliminates visual overlap of the curves, which is critically important for subsequent heat transfer analysis and verification of the second law of thermodynamics.

Nomenclature

Preprints.org (www.preprints.org) | NOT PEER-REVIEWED | Posted: 14 November 2025 doi:10.20944/preprints202511.1092.v1

A, ***B***, ***C***	sets of the ratios of the active bundle flows heat content to the total amount of heat transferred in the HEX, [W/W]
D	set of the active bundle flows parameters at the HEX outlet port
F	objective function
T	Temperature, [K]
P	Pressure, [bar]
Q	heat load, [W]
$\dot{m}$	mass rate, [kg/s]
n	number of HEX's sections
N	number of HEX's hot/cold flows
H	enthalpy, [W]
h	specific enthalpy, [J/kg]
S	entropy [W/K]
s	specific entropy [J/kg.K]
i	index of cross section: $\mathrm{i} \in [0, n]$
in	inlet port
max	maximum
min	minimum
i, *j*	hot flow index, $i \in [1..N^h]$; cold flow index, $j \in [1..N^h]$
out	outlet port
Greek symbols	
Δ	difference [--]
ε	effectiveness of heat exchanger [%]
φ	ratio of the active bundle flow heat content to the total amount of heat transferred in the HEX, [W/W]
ψ	ratio of the passive bundle flow heat content to the total amount of heat transferred in the HEX, [W/W]
Superscripts	
a	active
p	passive
h	hot
c	cold
id	ideal
Subscripts	
C, ***D***	indices of sets ***C*** and ***D***
act	actual
end	HEX outlet port
lim	limiting

 doi:10.20944/preprints202511.1092.v1

sorted	sorted
Abbreviations	
EOS	equation of state
HEX	heat exchanger
MFHEX	multi flow heat exchanger

References

1. Hohmann, E.C. (1971). *Optimum networks for heat exchange.* PhD Thesis, University of Southern California.
2. Linnhoff, B., & Flower, J.R. (1978). *Synthesis of heat exchanger networks: I. Systematic generation of energy optimal networks.* **AIChE Journal**, 24(4), 633–642.
3. Ghannadzadeh, M., et al. (2020). *Numerical modeling of multi-stream cryogenic heat exchangers.* **Cryogenics**, 108, 103087.
4. Wang, X., & Xu, Y. (2019). *Modeling and analysis of multi-stream heat exchangers for LNG processes.* **Energy**, 173, 1148–1160.
5. Bejan, A. (1997). *Entropy Generation Minimization.* CRC Press.
6. Lemmon, E.W., et al. (2018). *REFPROP 10.0: Reference Fluid Thermodynamic and Transport Properties.* NIST.
7. AspenTech (2022). *Aspen HYSYS 12.1 User Guide.* Aspen Technology Inc.